Effects of electron-correlation, spin-orbit coupling, and modified Becke-Johnson potential in double perovskites SrLaBB′O$_6$(B = Ni, Fe; B′ = Os, Ru)

Dinesh Kumar Yadav[a], Shalika Ram Bhandari[a,b], Bishnu Prasad Belbase[a], Gopi Chandra Kaphle[a,b], Dibya Prakash Rai[c], Madhav Prasad Ghimire[a,b,*]

[a] Central Department of Physics, Tribhuvan University, Kirtipur-44613, Kathmandu, Nepal
[b] Condensed Matter Physics Research Center, Butwal-11, Rupandehi, Nepal
[c] Physical Sciences Research Center (PSRC), Pachhunga University College, Mizoram University, Aizawl 796001, India

ABSTRACT

We investigate the electronic and magnetic properties of the newly synthesized SrLaBB′O$_6$ (B = Ni, Fe; B′ = Os, Ru) materials on the basis of density functional theory. Within local-density approximation (LDA), except for SrLaNiOsO$_6$, the studied materials are found to be metallic. Inclusion of electron-correlation effects (U) and spin-orbit coupling (SOC) leads to the opening of the band gap at the Fermi level (E_F) for all the selected materials. Additionally modified Becke-Johnson (TB-mBJ) potential has been used which is found to enhance the band gap of 0.62 eV and 0.59 eV in SrLaNiOsO$_6$ and SrLaNiRuO$_6$, respectively while remains metallic for the SrLaFeOsO$_6$. The magnetic ground state is found to be antiferromagnetic (AFM) for SrLaNiOsO$_6$ and SrLaNiRuO$_6$ consistent with the experimental observations. Replacing Ni by Fe in SrLaNiOsO$_6$ resulted in SrLaFeOsO$_6$. The ground state was found to be AFM. The co-operative effects of U and SOC opens a band gap (~0.03 eV) dictating the significant influence on SrLaFeOsO$_6$. On the otherhand, the Mott-insulating state is observed with a band gap opening of 0.33 eV and 0.58 eV for SrLaNiOsO$_6$ and SrLaNiRuO$_6$, respectively with the dominant contributions from the Os-$5d$ and Ru-$4d$ bands at and around the Fermi level. The magnetic anisotropy suggests an easy axis along the [0 0 1]-direction. Charge ordering is found to be prominent in these compounds. Our result agrees well with the experimental findings.

1. Introduction

The transition metal based double perovskites (DPs) are promising candidates due to the presence of *d*-orbitals which derives the fascinating chemical and physical properties. DPs exhibit diverse properties that includes metallicity, half-metallicity (HM), insulator, ferromagnetism (FM), ferrimagnetism (FIM) and antiferromagnetism (AFM) [1,2], etc. As such, DPs are potential candidates for spintronics application that resulted in faster data transfer and huge memory storage devices. The other reason being their structural stability and variation in the crystal structures from simple cubic to highly distorted monoclinic. The current research is mainly devoted to understand the structural, electronic and magnetic properties of such systems. There are two types of DP with chemical formula A$_2$BB′O$_6$ and AA′BB′O$_6$ respectively, where A, A′ are alkaline earth or rare earth elements and B, B′ are the transition elements. Among the family of DPs, the compound with Osmium-oxides are found to be rarely investigated due to the safety measures and difficulties in laboratory fabrication, as osmium

and oxygen are highly volatile, as reported in OsO$_4$[3]. However, the successful synthesis of osmium-oxide based DPs such as SrLaNiOsO$_6$ and SrLaNiRuO$_6$ from solid state reactions technique [4] motivates us to carry out thorough investigation and analyse their novel physical properties by means of first principles density functional theory (DFT) approach. It is interesting to note that the novel properties can be achieved by structural modification of A, A′ and B, B′ sites. For example, observation of a magnetic insulating state in Sr$_2$MOsO$_6$ (where M = Cu, Ni) [5], half semi-metallic AFM in Sr$_2$CrTO$_6$ (T = Os, Ru) [6], etc. AFM Mott-insulating state with an indirect band gap of 0.25 eV and 0.15 eV in Ca$_2$MgOsO$_6$ and Sr$_2$MgOsO$_6$, respectively under the effect of electron-correlations [7], and opening of the charge gap of ~0.17 eV in FM-Ba$_2$NiOsO$_6$ was found under the co-operative effect of electron-correlation and spin-orbit coupling (SOC) plays significant role. Furthermore, Ba$_2$NiOsO$_6$ shows metamagnetic transition and Dirac-Mott insulating FM state near 100 K [8]. An unusual superconducting behaviour has been observed in AOs$_2$O$_7$ (A = Cs, Rb and K) [9], magnetically driven metal-insulator transition (MIT) in NaOsO$_3$ at Neel

---

temperature (T_N) of 411 K [10]. The metallic $LiOsO_3$ shows ferroelectric type structural transition [11]. Moreover, DPs like Sr_2FeMoO_6 and Sr_2FeReO_6 are found to be HM-FIM which displays a giant tunneling magnetoresistance above room temperature [12–14]. Sr_2CrOsO_6 shows FIM order below Curie temperature ($T_C = \sim 725$ K), which seems to be the highest T_C known so far in DP oxides [15,16]. In addition, Sr_2ScOsO_6 shows AFM transition at 92 K [17] while Ca_2FeOsO_6 displays FIM transition at 320 K [18].

Recently, $SrLaNiIrO_6$ and $SrLaMgIrO_6$ have been studied and found to be AFM and weakly paramagnetic, respectively [19]. A first principles study reported the compensated HM, AFM semiconductor and HMF properties in Sr_2NiOsO_6, Sr_2FeOsO_6 and Sr_2NiRuO_6 respectively originated from the combine effect of electron correlation and SOC [3,20,21]. Likewise, a HM-FIM to HM-AFM transition is reported in Mott-Hubbard insulator type Pr_2MgIrO_6 when Sr is doped partially to the Pr sites. The materials are expected to be a novel candidate for spintronic applications [22].

Usually in DPs, LDA and or GGA is found to underestimate the band gap and magnetic moments. These can be corrected either by using LDA + U, GGA + U, or TB-mBJ potential [24,23,25]. Recently using TB-mBJ, electronic and magnetic properties are studied in DPs such as in A_2FeReO_6 (A = Sr, Ba), Sr_2XReO_6 (X = Cr, Mn, Fe, Ni) and Sr_2CrOsO_6, respectively [1,26,27]. The insulating state observed in experiment is confirmed for Sr_2XReO_6 (X = Mn, Ni) [26] and Sr_2CrOsO_6 [27], respectively, while HM state was observed for A_2FeReO_6 (A = Sr, Ba) and Sr_2XReO_6 (X = Cr, Fe) materials [1,26]. The accuracy of the band gap was found better as compared to LDA or GGA.

We recently noticed a newly synthesized $SrLaBB'O_6$ materials in which the magnetic atoms Ni (Fe) at B-site and Os (Ru) at B′-sites forms BO_6 and $B'O_6$ octahedra [4]. The octahedra in the structures exhibit a strong crystal distortion, which may provide a strong crystal field in addition to sizable strength of SOC. Due to the presence of heavy elements such as Os in DPs it induces larger SOC due to a large spatial extension of orbitals. This can lead to many desirable electronic and magnetic behaviors for technological applications. These intriguing combination are found in $SrLaBB'O_6$. This motivate us to explore the novel properties of this material, which are theoretically less studied due to their complex distribution of charges. The main goal here is to study the electronic and magnetic properties of these materials.

2. Crystal structures and computational details

The crystal structure of $SrLaBB'O_6$ as shown in Fig. 1 has a space group P2$_1$/n in which BO_6 and $B'O_6$ octahedra maintains the monoclinic structure [4,28]. There are three sort of oxygen atoms in B (B′)-O1, B (B′)-O2 and B (B′)-O3 (see in Fig. 1).

Here, we perform the DFT calculations to investigate the electronic and magnetic properties of $SrLaBB'O_6$. It is based on the full potential-linearized augmented plane wave plus local orbital (FP-LAPW + lo) method as implemented in the WIEN2k code [29]. The expansion in spherical harmonics was taken up to l = 10 for the radial wave function and charge densities and potentials were represented up to l = 6. The commonly used convergence criterion was chosen to be 7.0 of basis set $R_{MT} \times K_{max}$, where R_{MT} and K_{max} are smallest atomic sphere radius and plane wave cutoff respectively. The non-overlapping muffin-tin sphere radii (R_{MT}) of 2.34, 2.50, 2.06, 2.06, 2.02, 2.02 and 1.65 Bohr radius are used for Sr, La, Ni, Fe, Ru, Os and O respectively. The full Brillouin zone was sampled with 500 k-points ($8 \times 8 \times 6 k$-mesh). For the exchange-correlation potential local density approximation (LDA) [30] was chosen for the self-consistent calculations as this funtional is sufficient to address the results similar to GGA [31] functional. In addition, we use mBJ-potential proposed by Tran and Blaha [24,25] to resolve the band gap and related properties. The calculations are considered to be converged when the energy and charge convergence are less than 10^{-5} Ry and $10^{-4}e$, respectively. The Coulomb interactions (U) for the
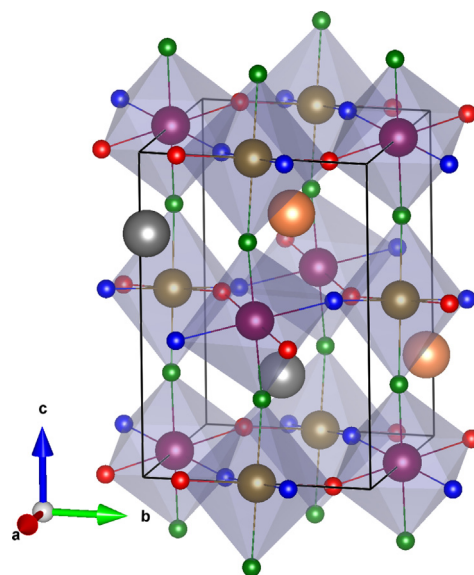

Fig. 1. Crystal structure of $SrLaNiOsO_6$ (colors in orange, grey, purple, gold, red, blue and green spheres corresponds to Sr, La, Ni, Os, O1, O2 and O3 atoms, respectively). (For interpretation of the references to colour in this figure legend, the reader is referred to the web version of this article.)

magnetic atoms Ni (Fe) and Os (Ru) are the system dependent quantity. The value of U generally separates the occupied and unoccupied states of the atoms. The values of U chosen in our calculations are based on the general values mostly used in literatures for Ni (Fe) and Os (Ru) atoms respectively. For $SrLaNiOsO_6$ and $SrLaFeOsO_6$, U_{Os} used are 0.5 eV and 1.5 eV, respectively. U_{Ni} is fixed to 5.0 eV for all the systems, similar to the previous reported values such as in Sr_2NiOsO_6 [3], Ca_2FeOsO_6 [32] and Sr_2FeOsO_6 [33], respectively. For $SrLaNiRuO_6$ we use $U_{Ru} = 0.5$ eV comparable to the values used in Sr_2NiRuO_6 [21]. Since Ru-$4d$ and Os-$5d$ orbitals are delocalized compared to Ni-$3d$ orbitals, the chosen values of Os (Ru) are small. In the present calculations, $U_{eff} = U - J$ with J fixed to zero in LDA + U. The SOC was included as the second variational step using the scalar-relativistic eigenfunctions as a basis [34]. Note that the experimental parameters with P2$_1$/n consists only of 6 equivalent atoms with one magnetic atoms at the B and B′ sites. In order to obtain the four different magnetic configurations, a $1 \times 1 \times 1$ supercell was generated which corresponds to a total of 20 atoms with two each of in-equivalent magnetic atoms at the B and B′ sites.

3. Results and discussion

The experimental lattice parameters measured from neutron powder diffraction at 10 K [4] has been optimized. The obtained values are used for electronic and magnetic state calculations. We calculate the total energies for four possible magnetic configurations with alignments of inequivalent atoms Ni1, Ni2, Os1 and Os2 in $SrLaNiOsO_6$ as follows: one FM (↑↑↑↑), two AFM (AF1-↑↓↑↓, AF2-↑↓↓↑) and one FIM (↑↑↓↓) as shown in Fig. 2. The AF2 (↑↓↓↑) magnetic configuration is found to be the ground states consistent with the experimental observation [4] indicating the AFM configuration at ground state. The energy difference to the next lowest order (FIM) is ~8 meV within LDA calculations. This shows the competing ground state among the AF states with a possibility of canting AFM state. Similarly, the ground state is AF2 for $SrLaFeOsO_6$ with energy difference of ~21 meV with respect to the next lowest order (AF1). In contrary, $SrLaNiRuO_6$ is found to have the AF1 ground state which competes with the AF2-state with an energy difference ~31 meV. $SrLaNiRuO_6$ undergo long range magnetic interaction by considering (Ni^{2+}-Ni^{2+} and Ru^{5+}-Ru^{5+}) AF coupling [35] consistent with our findings.
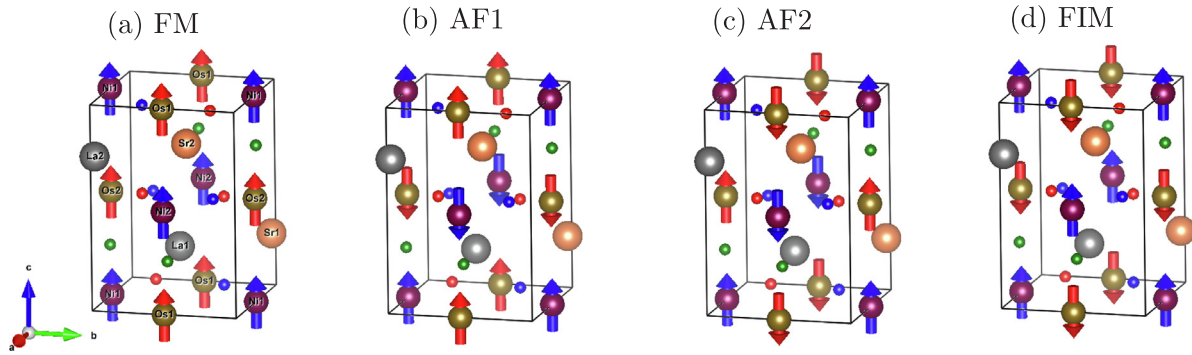
Fig. 2. Magnetic configuration of SrLaNiOsO$_6$: (a) FM, (b) AF1, (c) AF2, and (d) FIM. The blue and red arrows within the crystal structure indicates the direction of Ni and Os spins along the direction of easy axis [0 0 1].
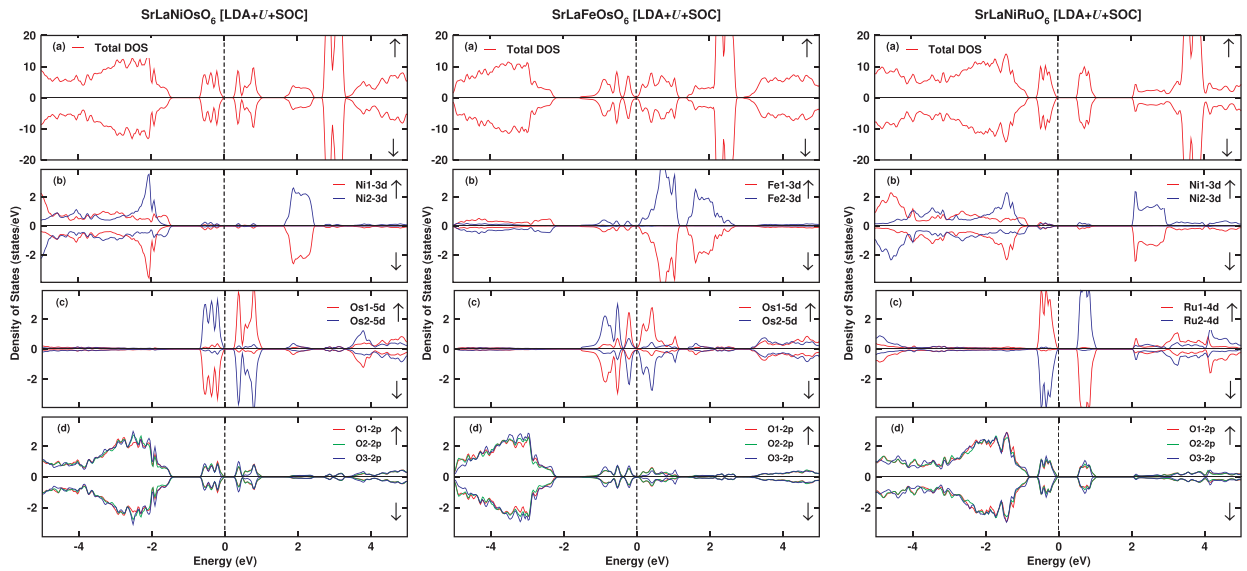

Fig. 3. (a) Total and partial DOS of (b) B (Ni, Fe), (c) B′ (Os, Ru), and (d) O-atoms in spin up (↑) and spin down (↓) channel for SrLaBB′O$_6$ within LDA + U + SOC functional. The vertical dotted line indicates the $E_F = 0$.

Fig. 3 shows the density of state (DOS) within LDA + U + SOC functional for SrLaNiOsO$_6$, SrLaFeOsO$_6$ and SrLaNiRuO$_6$ with (a) the total DOS and partial DOS of (b) Ni (Fe)-3d states, (c) Ru-4d (Os-5it d) states and (d) O-2p states, respectively. SrLaNiOsO$_6$ within LDA calculations shows a band gap of 0.04 eV with symmetric DOS in both spin up and spin down channels. The presence of transition elements Ni and Os derive strong correlation effect which is ignored in LDA or GGA functionals. The implementation of DFT + U approximation includes the electron-correlation (U) to get more accurate results close to experimental finding and the band gap is opened to 0.44 eV. As heavy atoms are strongly influenced by SOC, it has been applied to examine the effect of spin quantization along [1 0 0], [0 1 0], [0 0 1], [1 1 1]-directions. We found the easy axis along [0 0 1]-direction. Considering SOC in SrLaNiOsO$_6$ the band gap has been reduced to 0.33 eV, which is close agreement with the recent experimentally obtained activation energy of 0.35 eV at 300 K [36]. Thus, the combined effect of U and SOC in SrLaNiOsO$_6$ enhanced the result significantly.

We further consider the mBJ effects in SrLaBB′O$_6$ (B = Ni, Fe; B′ = Os, Ru). A significant increase in the exchange splitting of Ni (Fe)-3d, Ru-4d and Os-5d states has been noted around (E_F). As a result large value of exchange splitting is seen in Ni-3d state as compared to Fe-3d states. Figs. 5 and 6 shows the DOS and band structure using mBJ potential for the selected system. It is interesting to note that the band gap which remains 0.04 eV in LDA rises to 0.62 eV when mBJ is applied in SrLaNiOsO$_6$, hence over-estimating the experimetal band gap (0.35 eV).

The splitting of the d-state electrons from different transition metals due to mBJ are found around the Fermi level (E_F) (see Fig. 5 (b), (c)).

Similarly, SrLaNiRuO$_6$ which shows metallic state in LDA, is found to have a band gap of 0.51 eV and 0.58 eV when U and U + SOC is applied. Interestingly the band gap increases for this particular system within SOC, while an another group in their calculation within LSDA + U + SOC reported insignificant effect of SOC in SrLaNiRuO$_6$ [35]. Further we observe a noticable changes on the Ru-4d bands, in which it splits near E_F as can be seen in the DOS and band structure plots (see Fig. 3 and Fig. 4). With mBJ, the band gap is found to be 0.59 eV as can be seen in Figs. 5 and 6 with the detail informations on magnetic moments in Table 1. and 2, respectively.

Likewise, SrLaFeOsO$_6$ is found to be metallic for U_{Os} as large as 2 eV. With SOC, a tiny band gap of 0.03 eV is induced resulting in the semiconducting state. Unfortunately, the system remains metallic even when the mBJ potential is used. The related band structures for all the compounds shows an indirect band gap as shown in Fig. 4 and Fig. 6. The calculated band gaps suggest that SrLaNiOsO$_6$, SrLaFeOsO$_6$ and SrLaNiRuO$_6$ are Mott-insulators. The major contributions to the DOS around E_F are from the Os-5d and Ru-4d oritals.

From the DOS plots shown in Fig. 3 for all the three compounds, we observe that the main contribution near E$_F$ are from the d states of Ni, Fe, Os and Ru respectively hybridizing strongly with the oxygen 2p states. The spin polarized DOS shows symmetric behavior in spin up and spin down channel resulting in zero effective magnetic moment.
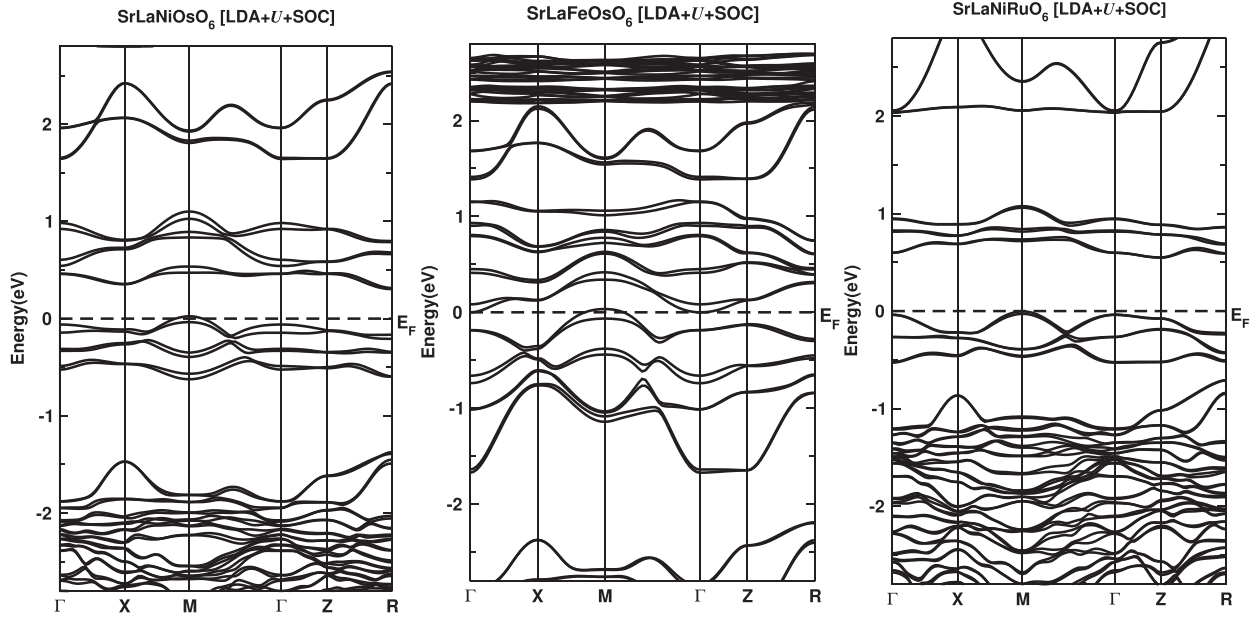
Fig. 4. Band structures of the SrLaBB′O$_6$ (B = Ni, Fe; B′ = Os, Ru) within LDA + U + SOC functional. Dashed horizontal lines at zero energy corresponds to E_F.

The strong hybridization observed between oxygen $2p$ bands and d states of Ni (Fe)-$3d$ and Ru-$4d$ (Os-$5d$) around E_F are caused by octahedral distortion.

The band structure for the studied compounds are shown in Fig. 4 and Fig. 6 where Ru-$4d$ (Os-$5d$) bands that are dominant near E_F splits due to finite strength of SOC. This resulted in the insulating behaviour with an indirect band gap for these systems.

In SrLaNiOsO$_6$ charge state of Ni is 2+ with $3d - t_{2g}^6 e_g^2$ configuration and that of Os is 5+ with $5d - t_{2g}^3 e_g^0$ respectively, as shown in Fig. 7. When comparing the partial DOS features around E_F (see Figs. 3 and 5) the major contributions are from Ni-$3d$ and Os-$5d$ characters with some mixing from the O-$2p$ states. As can be seen, the Ni-$3d$ states are fully occupied (d^5) in the spin up channel while only the t_{2g} occupied in spin down channel, whereas for Os only t_{2g} states are occupied in spin one of the spin channel with the remaining d-states empty in both spin channels. This lead to charge state of Ni^{2+} with d^8 occupancy and Os^{5+} with d^3 occupancy.

Moving onto SrLaFeOsO$_6$, the charge state of Fe becomes 3+ with $3d - t_{2g}^3 e_g^2$ and of Os is 4+ with $5d - t_{2g}^2 e_g^0$ configuration as shown in Fig. 7. From the partial DOS calculations we found that Fe-$3d$ states are fully occupied in the spin up channel and empty in spin down channel,

while only t_{2g} is occupied in spin down channel leaving all the remaining bands empty in both spin channels. Likewise, the charge state of Ni is 2+ with d^8 and that of Ru is 5+ with d^3 configurations in SrLaNiRuO$_6$. This shows the similar features as discussed above for SrLaNiOsO$_6$. From the above discussion it clearly indicates a change in the charge transfer from B to B′ when an atom are interchanged.

We further investigate the magnetic behavior in selected systems as tabulated in Table 1 and Table 2. As from the ionic picture for SrLaNiOsO$_6$, Ni and Os atoms carry spin magnetic moments of 2 μ_B and 3 μ_B each, while from DFT resulted Ni = 1.74 μ_B and Os = 1.36 μ_B respectively. The moment are found to increase when applying U while due to SOC, Os-moment decreases. Inclusion of mBJ is found to increase the spin magnetic moment of Ni and Os contradicting with the LDA but are closer to LDA + U and LDA + U + SOC results. Similar trends are noticed, for other materials as well which indicates the better agreement of the magnetic moments. When Fe is doped to Ni-site, the ionic magnetic moments rises to 5 μ_B and 2 μ_B each for Fe and Os respectively. The calculated moments are 4.04 μ_B and 0.88 μ_B for Fe and Os atoms with SOC included.

In SrLaNiRuO$_6$ although the ionic magnetic moments are same as of the SrLaNiOsO$_6$, the calculated magnetic moment of Ni and Ru are 1.70
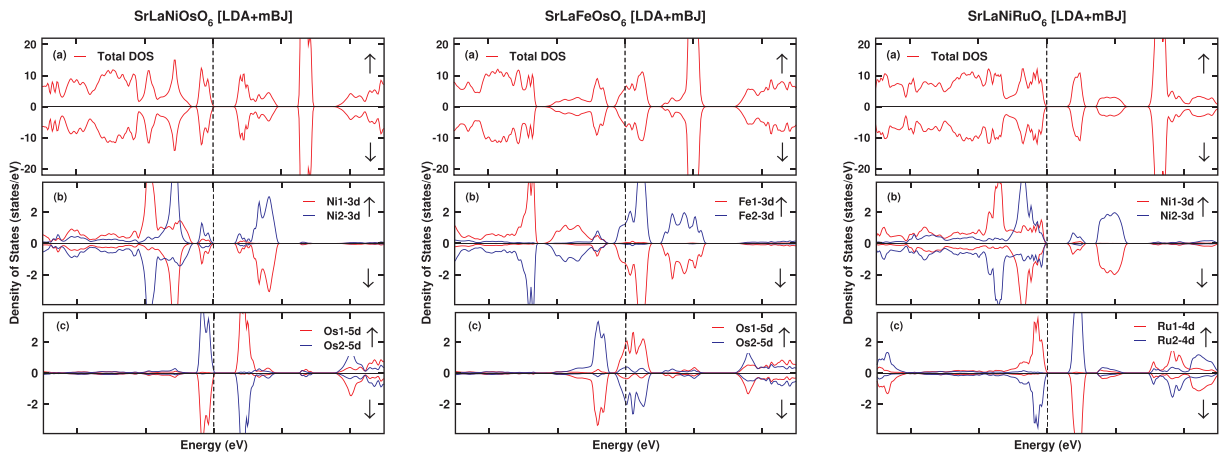

Fig. 5. (a) Total and partial DOS of (b) B (Ni, Fe), and (c) B′ (Os, Ru) in spin up (↑) and spin down (↓) channel for SrLaBB′O$_6$ within LDA + mBJ functional. The vertical dotted line indicates $E_F = 0$.
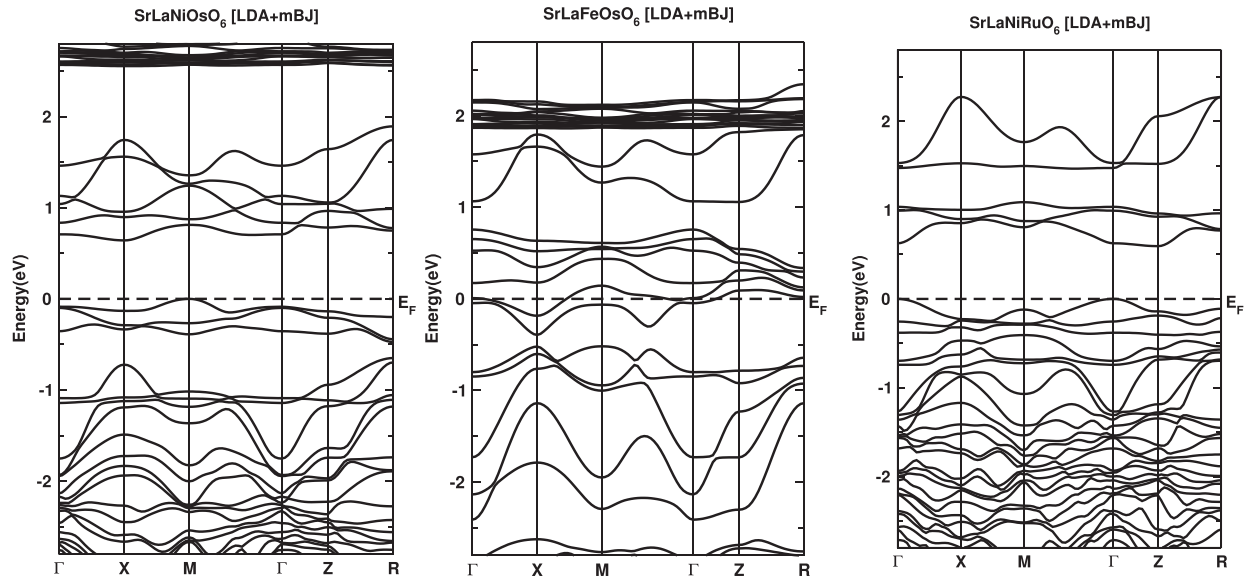
Fig. 6. Band structures of the SrLaBB'O$_6$ (B = Ni, Fe; B'= Os, Ru) within LDA + mBJ functional. Dashed horizontal lines at zero energy corresponds to the Fermi level.

Table 1
Calculated spin magnetic moments (in μ_B) of B (Ni, Fe), B' (Os, Ru), 3 inequivalent oxygens and the gap 'E$_g$' (eV) for SrLaBB'O$_6$.

Site	SrLaNiOsO$_6$		SrLaFeOsO$_6$		SrLaNiRuO$_6$	
	LDA	LDA + mBJ	LDA	LDA + mBJ	LDA	LDA + mBJ
B	1.38	1.57	3.54	3.64	1.49	1.60
B'	1.36	1.58	0.77	1.17	1.54	1.70
O1	0.06	0.09	0.02	0.02	0.19	0.19
O2	0.06	0.08	0.02	0.01	0.19	0.20
O3	0.16	0.17	0.14	0.18	0.05	0.08
E$_g$	0.04	0.62	Metallic	Metallic	Metallic	0.59

Fig. 7. Schematic picture of the occupancies of Ni, Fe, Os, and Ru d states in SrLaNiOsO$_6$ (top), SrLaFeOsO$_6$ (middle) and SrLaNiRuO$_6$ (bottom) as obtained from the DFT calculations.

μ_B and 1.65 μ_B respectively. This difference in the magnetic moment is due to the partial charge transfer of moment to inequivalent oxygens via charge transfer between B-O and B'-O site atoms in addition to octahedral distortions.

With consideration of SOC in SrLaNiOsO$_6$, orbital moment is induced on Ni and Os are antiparallel to that of the spin magnetic moment as tabulated in Table 2. This results in the reduction of the net magnetic moment. Additionally, orbital moment of Ni is relatively large (i.e., 0.22 μ_B) as compared to the Os atoms with 0.15 μ_B. The reason for large orbital moment is caused by the larger orbital coupling of Ni with the oxygen atoms in comparison to Os with the oxygen atoms. Similar features had been reported in Ca$_2$CoOsO$_6$ [37]. Due to hybridization with Ni and Os, oxygen also gain small magnetic moment and polarization is mainly found on $2p$-orbitals. For the case of SrLaFeOsO$_6$ the
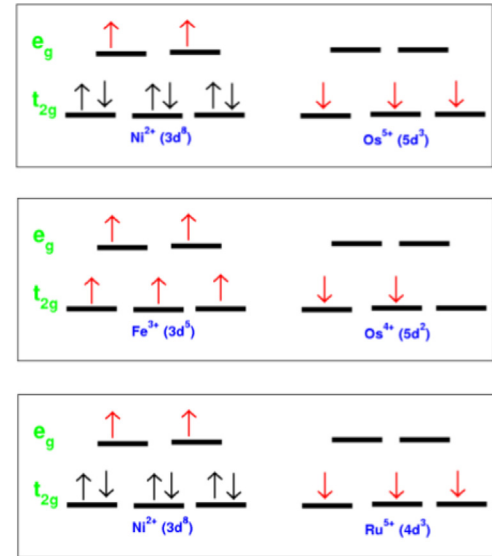
orbital moment are 0.09 μ_B and 0.22 μ_B respectively similar to Sr$_2$FeOsO$_6$ [20]. In SrLaNiRuO$_6$, the orbital magnetic moment of Ni and Ru are 0.24 μ_B and 0.03 μ_B, analogous to Sr$_2$NiRuO$_6$ [21] and

Table 2
Calculated spin magnetic moments (in μ_B) of B (Ni, Fe), B' (Os, Ru), 3 oxygens and band gap 'E$_g$' (eV). The calculated orbital moments at B and B' sites are shown within parentheses for SrLaBB'O$_6$.

Site	SrLaNiOsO$_6$		SrLaFeOsO$_6$		SrLaNiRuO$_6$	
	LDA + U	LDA + U + SOC	LDA + U	LDA + U + SOC	LDA + U	LDA + U + SOC
B	1.68	1.68(0.22)	4.02	4.04(0.09)	1.70	1.70(0.24)
B'	1.52	1.36(0.15)	1.09	0.88(0.23)	1.66	1.65(0.03)
O1	0.09	0.08	0.02	0.01	0.16	0.16
O2	0.09	0.08	0.01	0.02	0.16	0.16
O3	0.14	0.13	0.14	0.12	0.08	0.08
E$_g$	0.44	0.33	Metallic	0.03	0.51	0.58

Sr_2CrRuO_6 [6].

4. Conclusions

On the basis of DFT calculations, we found the semiconducting behavior in $SrLaBB'O_6$ (B = Ni, Fe; B′ = Os, Ru) materials. All the studied materials having monoclinic structure are found to have the antiferromagnetic ground state with their easy axis oriented along the [0 0 1]-direction. $SrLaNiOsO_6$ and $SrLaNiRuO_6$ shows Mott-like insulating state under the co-operative effect of Coulomb interaction, SOC in addition to the crystal field with a band gap of 0.33 eV and 0.58 eV, respectively. When Ni is replaced with Fe in $SrLaNiOsO_6$, the electronic behavior shows metallic state within LDA + U. Upon inclusion of SOC, a tiny band gap of 0.03 eV has been obtained in $SrLaFeOsO_6$. Similar to the effects of correlation, the band gap are found to be 0.62 eV in $SrLaNiOsO_6$ and 0.59 eV in $SrLaNiRuO_6$, while remains metallic in $SrLaFeOsO_6$. For all the systems, the net calculated magnetic moment is zero per unit cell with sizable spin and orbital magnetic moments. Our results are found consistent with the available experimental finding of Morrow et. al. [4]. Charge ordering is found to be prominent in these compounds. From this study $SrLaFeOsO_6$ and $SrLaNiRuO_6$ are predicted to be a semiconductor similar to the parent material $SrLaNiOsO_6$. Further study on these type of materials are strongly suggested by varying the BB′ sites, to tune the novel properties useful for spintronics and quantum magnetic devices fabrication.

CRediT authorship contribution statement

Dinesh Kumar Yadav: Conceptualization, Investigation, Methodology, Visualization, Writing - original draft, Writing - review & editing. **Shalika Ram Bhandari:** Investigation, Methodology, Visualization, Writing - original draft. **Bishnu Prasad Belbase:** Investigation, Writing - original draft. **Gopi Chandra Kaphle:** Resources, Writing - original draft, Project administration, Supervision. **Dibya Prakash Rai:** Resources, Formal Analysis. **Madhav Prasad Ghimire:** Conceptualization, Investigation, Methodology, Software, Validation, Visualization, Project administration, Resources, Supervision, Writing - original draft, Writing - review & editing.

Conflict of interest

There is no conflict of interest.

Acknowledgments

References

[1] D.P. Rai, A. Shankar, M.P. Ghimire, R.K.Thapa Sandeep, Comp. Mat. Sc. 101 (2015) 313.
[2] M.T. Anderson, K.B. Greenwood, G.A. Taylor, K.R. Poeppelmeier, Prog. Solid State Ch. 22 (1993) 197.
[3] W. Song, E. Zhao, J. Meng, Z. Wu, J. Chem. Phys. 130 (2009) 114707.
[4] R. Morrow, M.A. McGuire, Jiaqiang, P.M. Woodward, Inorg. Chem. 57 (2018) 2989.
[5] C. Tian, A.C. Wibowo, H.C. zur Loye, M.H. Whangbo, Inorg. Chem. 50 (2011) 4142.
[6] K.W. Lee, W.E. Pickett, Phys. Rev. B 77 (2008) 115101.
[7] Y. Yahua, H.L. Feng, M.P. Ghimire, Y. Matsushita, Y. Tsujimoto, J. He, M. Tanaka, Y. Katsuya, K. Yamaura, Inorg. chem. 54 (2015) 3422.
[8] H.L. Feng, S. Calder, M.P. Ghimire, Y. Yuan, Y. Shirako, Y. Tsujimoto, Y. Matsushita, Z. Hu, C.Y. Kuo, L.H. Tjeng, T.W. Pi, Y.L. Soo, J. He, M. Tanaka, Y. Katsuya, M. Richter, K. Yamaura, Phys. Rev. B 94 (2016) 235158.
[9] Z. Hiroi, J. Yamaura, K. Hattori, J. Phys. Soc. Jpn. 81 (2012) 011012.
[10] S. Calder, V.O. Garlea, D.F. McMorrow, M.D. Lumsden, M.B. Stone, J.C. Lang, J.W. Kim, J.A. Schlueter, Y.G. Shi, K. Yamaura, Y.S. Sun, Y. Tsujimoto, A.D. Christianson, Phys. Rev. Lett. 108 (2012) 257209.
[11] Y.G. Shi, Y.F. Guo, X. Wang, A.J. Princep, D. Khalyavin, P. Manuel, Y. Michiue, A. Sato, T. Tsuda, S. Yu, M. Arai, Y. Shirako, M. Akaogi, N.L. Wang, K. Yamaura, A.T. Boothroyd, Nat. Mater. 12 (2013) 1023.
[12] K.I. Kobayashi, T. Kimura, H. Sawada, K. Terakura, Y. Tokura, Nature (London) 395 (1998) 677.
[13] K.I. Kobayashi, T. Kimura, Y. Tomioka, H. Sawada, K. Terakura, Y. Tokura, Phys. Rev. B 59 (1999) 11159.
[14] M. Sakai, A. Massuno, D. Kan, M. Hashisaka, K. Takata, A. Azuma, M. Takano, Y. Shimakawa, Appl. Phys. Lett. 90 (2007) 072903.
[15] Y. Krockenberger, K. Mogare, M. Reehuis, M. Tovar, M. Jansen, G. Vaitheeswaran, V. Kanchana, F. Bultmark, A. Delin, F. Wilhelm, A. Rogalev, A. Winkler, L. Alff, Phys. Rev. B 75 (2007) 020404.
[16] O.N. Meetei, O. Erten, M. Randeria, N. Trevedi, P. Woodword, Phys. Rev. Lett. 110 (2013) 087203.
[17] A.E. Taylor, R. Morrow, D.J. Singh, S. Calder, M.D. Lumsden, P.M. Woodward, A.D. Christianson, Phys. Rev. B 91 (2015) 100406.
[18] H.L. Feng, M. Arai, Y. Matsushita, Y. Tsujimoto, Y. Guo, C.I. Sathish, X. Wang, Y.H. Yuan, M. Tanaka, K. Yamaura, J. Am. Chem. Soc. 136 (2014) 3326.
[19] K.K. Wolff, S. Agrestini, A. Tanaka, M. Jansen, L.H. Tjeng, Z. anorg. allg. Chem. 643 (2017) 2095.
[20] J. Wang, N. Zu, X. Hao, Y. Xu, Z. Li, Z. Wu, F. Gao, Physica Status Solidi-R 8 (2014) 776.
[21] S.E.A. Yousif, O.A. Yassin, J. Alloy. Compd. 506 (2010) 456.
[22] M.P. Ghimire, L.H. Wu, X. Hu, Phys. Rev. B 93 (2016) 134421.
[23] A.D. Becke, M.R. Roussel, Phys. Rev. A 39 (1989) 3761.
[24] F. Tran, P. Blaha, Phys. Rev. Lett. 102 (2009) 226401.
[25] A.D. Becke, E.R. Johnson, J. Chem. Phys. 124 (2006) 221101.
[26] G. San-Dong, Eur. Phys. J. B 88 (2015) 82.
[27] G. San-Dong, Chin. Phys. Lett. 31 (2014) 017101.
[28] K. Momma, F. Izumi, J. Appl. Crystallogr. 44 (2011) 1272.
[29] P. Blaha, K. Schwarz, G.K.H. Madsen, D. Kvasnicka, J. Luitz, WIEN2k (version 14.2), An Augmented Plane Wave + Local Orbitals Program for Calculating Crystal Properties, Technische Universität Wien, Vienna, Austria, 2001.
[30] V.I. Anisimov, I.V. Solovyev, M.A. Korotin, M.T. Czyzyk, G.A. Sawatzky, Phys. Rev. B 48 (1993) 16929.
[31] J.P. Perdew, K. Burke, M. Ernzerhof, Phys. Rev. Lett. 77 (1996) 3865.
[32] M.P. Ghimire, X. Hu, Mater. Res. Express 3 (2016) 106107.
[33] S. Kanungo, B. Yan, M. Jansen, C. Felser, Phy. Rev. B 89 (2014) 214414.
[34] J. Kuneš, P. Novâk, M. Diviš, P.M. Oppeneer, Phys. Rev. B 63 (2001) 205111.
[35] X. Ou, F. Fan, X. Chen, T. Li, L. Jiang, A. Stroppa, X. Ouyang, H. Wu, Europhys. Lett. 123 (2018) 57003.
[36] H.L. Feng, W. Schnelle, L.H. Tjeng, M. Jansen, Solid State Commun. 243 (2016) 49.
[37] R. Morrow, K. Samanta, T.S. Dasgupta, J. Xiong, J.W. Freeland, D. Haskel, P.M. Woodward, Chem. Mater. 28 (2016) 3666.